

# Digital Metering of Power Components According to IEEE Standard 1459-2000 Using the Newton-Type Algorithm

Vladimir V. Terzija, *Senior Member, IEEE*, Vladimir Stanojević, Marjan Popov, *Senior Member, IEEE* and Lou van der Sluis, *Senior Member, IEEE*

**Abstract**—In this paper, a new two-stage Newton-Type Algorithm for the measurement of power components according to the IEEE Standard 1459-2000 is presented. To estimate their spectra and fundamental frequency, in the first stage, the current and voltage signals are processed, whereas in the second stage, the power components are calculated based on the results obtained in the first stage. The algorithm considers the frequency as an unknown parameter and simultaneously estimates it with the input signal spectrum. Through this, the algorithm becomes insensitive to frequency changes and the problem becomes non-linear. The algorithm performance is tested using computer-simulated and laboratory tests.

**Index Terms**—IEEE Standard 1459-2000, nonlinear estimation, power measurement, power systems, transient processes.

## NOTATION

The following notation will be used in this paper:

$\mathbf{h}(\hat{\mathbf{x}}_i, t) - (N \cdot 1)$	Vector of nonlinear functions determined by the signal model.
$\hat{\mathbf{x}}_i$	Estimated vector of unknowns in the $i$ th iteration.
$\xi(t)$	Zero-mean random noise.
$\omega$	(Fundamental) Angular velocity.
$\sigma$	Noise standard deviation.
$\omega_m$	Discretized (fundamental) angular velocity.
$\varphi_k$	Phase angle of the $k$ th harmonic.
$\theta_k$	Phase angle between $V_k$ and $I_k$ .
$\varphi_{km}$	Discretized phase angle of the $k$ th harmonic.
$\xi_m$	Discretized random noise.
$f_s$	Sampling frequency.
$h(\mathbf{x}, t)$	Nonlinear function modeling the input signal.
$I_{e,\text{RMS}}$	RMS effective current.

$I_{e1,\text{RMS}}$	Fundamental rms effective current.
$\mathbf{j}$	Arbitrary row of the Jacobian.
$\mathbf{J}$	Jacobian matrix (matrix of partial derivatives of the signal model with respect to unknown parameters).
$\mathbf{J}^\#$	Left pseudoinverse of the Jacobian matrix.
$M$	Highest-order harmonic presented in the signal.
$N$	Nonactive power.
$N$	Number of samples belonging to a data window.
$n$	Number of unknowns and the order of the model.
$P$	Active power.
$P_1$	Fundamental (50 or 60 Hz) active power.
$P_H$	Harmonics active power.
$Q_1$	Fundamental reactive power.
$Q_B$	Budeanu's reactive power.
$S$	Apparent power.
$S_1$	Fundamental apparent power.
$S_e$	Effective three-phase apparent power.
$S_{eN}$	Nonfundamental effective apparent power.
$S_N$	Nonfundamental apparent power.
SNR	Signal-to-noise ratio.
$t$	Time.
$t_{\text{cnv}}$	Convergence period.
$T_{\text{dw}}$	Length of data window.
$t_m$	Discretized time.
$T_s$	Sampling period.
$\mathbf{v}$	$(N \cdot 1)$ measurement vector.
$v(t)$	Instantaneous voltage at time $t$ .
$V_0$	Magnitude of the dc component.
$V_{0m}$	Discretized magnitude of the dc component.
$V_{e,\text{RMS}}$	RMS effective voltage.
$V_{e1,\text{RMS}}$	Fundamental rms effective voltage.
$V_k$	Magnitude of the $k$ th harmonic.
$V_{km}$	Discretized magnitude of the $k$ th harmonic.
$v_m$	Discretized value of the signal
$V_{\text{RMS}}$ and $I_{\text{RMS}}$	RMS values of voltages and currents.
$\mathbf{x}$	Vector of unknown parameters to be estimated.
$\mathbf{x}_m$	Discretized vector of unknown parameters to be estimated.

Manuscript received October 6, 2006; revised June 20, 2007.

V. Terzija is with the School of Electrical and Electronic Engineering, The University of Manchester, M60 1QD Manchester, U.K. (e-mail: terzija@ieee.org).

V. Stanojević is with the Imperial College London, SW7 2AZ London, U.K. (e-mail: v.stanojevic@imperial.ac.uk).

M. Popov and L. van der Sluis are with the Power System Laboratory, Delft University of Technology, 2628 Delft, The Netherlands (e-mail: M.Popov@ieee.org; L.vanderSluis@ewi.tudelft.nl).

Color versions of one or more of the figures in this paper are available online at <http://ieeexplore.ieee.org>.

Digital Object Identifier 10.1109/TIM.2007.908235

## I. INTRODUCTION

**T**HE INCREASED use of power electronics and electronic- and microprocessor-based devices, and the existence of nonlinear loads in today's power system, contribute to the unwanted distortion of voltage and current waveforms due to harmonics [1]. This creates the need for a more accurate method of measuring the power components in the presence of signal distortions. In [2], it is recommended to replace the existing solid-state energy meters with digital meters. The functionality of digital meters is determined by the quality of the input signals, the quality of the digital components, and the selection of the numerical algorithm for input signal processing. The fast Fourier technique (FFT) [3] is commonly applied for harmonic component extraction. In [4], its application is presented. However, the FFT optimal functionality is obtained if the frequency of the processed input signals is constant (e.g., 50 or 60 Hz). Kalman-filtering-based methods [5], [6] can also be used for harmonic component extraction. The problem of frequency deviations is tackled by implementing the extended Kalman filter. The statistical properties of the processed signals are required for the optimal estimation of unknown signal parameters (e.g., frequency, spectrum, etc.). They are often difficult to determine, so estimators *not* including signal statistics would be an attractive alternative. In this paper, the Newton-Type Algorithm (NTA) is implemented to estimate the unknown signal parameters. Starting with the assumption that the frequency of the input signal is not constant but variable in time, the list of unknown parameters is extended with the signal frequency. By doing this, the measurement problem becomes nonlinear, and strategies of nonlinear parameter estimation should be applied.

In the first stage of the algorithm, the NTA is implemented for harmonic components and signal frequency estimation. In the second stage, the power components are being calculated. For this purpose, the suitable power definitions are assumed in advance.

In the past, a number of papers dedicated to the definition of electrical power components have been published [7]–[10]. In this paper, the power component definitions given in IEEE Standard 1459-2000 [11]–[13] are an integral part of the numerical algorithm for power component measurement.

First, the NTA is presented. Next, the power definitions from IEEE Standard 1459-2000 and the block diagram of the complete two-stage numerical algorithm are outlined. This paper ends with the testing of the algorithm, i.e., computer-simulated signals (pure test signals with a known structure) and signals obtained in the power system laboratory are processed, and the results are evaluated.

## II. NTA ALGORITHM DEVELOPMENT

Let us assume the following observation model of the input voltage (or current) signal digitized at the measurement device location:

$$v(t) = h(\mathbf{x}, t) + \xi(t) \quad (1)$$

where  $v(t)$  is an instantaneous voltage at time  $t$ ,  $\xi(t)$  is a zero-mean random noise,  $\mathbf{x}$  is a suitable parameter vector, and  $h(\cdot)$

is a nonlinear function expressed as

$$h(\mathbf{x}, t) = V_0 + \sum_{k=1}^M V_k \sin(k\omega t + \varphi_k). \quad (2)$$

For the generic model (2), a suitable vector of unknown parameters is given by

$$\mathbf{x} = [V_0, \omega, V_1, \dots, V_M, \varphi_1, \dots, \varphi_M]^T \quad (3)$$

where  $V_0$  is the magnitude of the dc component;  $M$  is the highest order of the harmonics presented in the signal;  $\omega$  is the fundamental angular velocity equal to  $2\pi f$ , where  $f$  is the frequency;  $V_k$  is the magnitude of the  $k$ th harmonic; and  $\varphi_k$  is the phase angle of the  $k$ th harmonic ( $k = 1, \dots, M$ ). The equivalent signal model can also be used to describe the current signal.

The adopted signal model is a nonlinear function of the unknown frequency, so the application of a nonlinear estimation technique is required. In comparison to the linear estimation, this is a more complex problem. The benefit of introducing the signal frequency in the list of unknown parameters is the expected algorithm insensitivity to frequency changes (both small and large). Large interconnected electric power systems are normally operated in such a state that its frequency changes lie in a narrow band ( $\pm 0.05$  Hz) and the rate of change is almost negligible. Contrary, during and after a fault in the system, i.e., during the large power imbalances in the system, the change of the frequency and its rate of change are larger, and this strongly influences the accuracy of the existing algorithms for power measurement and for measurement in general.

If the input signal is uniformly sampled with the sampling frequency  $f_s$  and the sampling period  $T_s = 1/f_s$ , then the value of  $t$  at a discrete time index is given by  $t_m = mT_s$ , and the following discrete representation of the signal model can be used:

$$v_m = h(\mathbf{x}_m, t_m) + \xi_m, \quad m = 1, 2, 3, \dots \quad (4)$$

$$h(\mathbf{x}_m, t_m) = V_{0m} + \sum_{k=1}^M V_{km} \sin(k\omega_m t_m + \varphi_{km}) \quad (5)$$

and all the unknown parameters from (3) now have the subscript  $m$ .

The number of unknowns that determines the order of the model is  $n = 2M + 2$ . The order can be reduced by taking simplified models, i.e., by reducing the value of  $M$ . In the most simple case, the model that contains only the fundamental harmonic has the order  $n = 3$  and  $\mathbf{x} = [\omega, V_1, \varphi_1]^T$ . This model can be applied to process pure sinusoidal input signals. The model selection depends on the application, i.e., on the features of the processed input signal and the data acquisition digital system.

The input signals are sampled during a finite period of time called a *data window*.  $N$  samples belonging to the data window result in a set of  $N$  ( $N \geq n = 2M + 2$ ) nonlinear equations given by (4) and (5) in  $n$  unknowns. Now the problem is to

solve the overdetermined system of nonlinear equations, i.e., to estimate the unknown model parameters.

In [14], the NTA for the simultaneous estimation of voltage phasors and power system frequency is described. It is derived under the assumption that the input voltage is a pure sine wave. In this paper, in which a problem of power measurement is addressed, the distortion of input signals should be taken into account in the way as described in (2). The NTA algorithm belongs to the family of nonrecursive nonlinear estimators. The key relation of the NTA algorithm is

$$\hat{\mathbf{x}}_{i+1} = \hat{\mathbf{x}}_i + (\mathbf{J}_i^T \mathbf{J}_i)^{-1} \mathbf{J}_i^T (\mathbf{v} - \mathbf{h}(\hat{\mathbf{x}}_i, t)) \quad (6)$$

where  $i$  is an iteration index,  $\hat{\mathbf{x}}$  is the estimated vector,  $\mathbf{J}_i^\# = (\mathbf{J}_i^T \mathbf{J}_i)^{-1} \mathbf{J}_i^T$  is referred to as the left pseudoinverse of the Jacobian  $\mathbf{J}_i$ ,  $\mathbf{v}$  is an  $(N \cdot 1)$  measurement vector,  $\mathbf{h}(\hat{\mathbf{x}}_i, t)$  is an  $(N \cdot 1)$  vector of nonlinear functions determined by the assumed mathematical description of the input signal, and  $N$  is the number of samples from the data window. The Jacobian matrix  $\mathbf{J}$  is an  $(N \cdot n)$  matrix, and its elements are the partial derivatives of the signal (2). Let us denote with  $\mathbf{j}$  an arbitrary row of the Jacobian

$$\mathbf{j} = [j_1, j_2, j_3, \dots, j_{2+2M}] \quad (7)$$

$$j_1 = \frac{\partial h(\mathbf{x})}{\partial V_0} = 1 \quad (8)$$

$$j_2 = \frac{\partial h(\mathbf{x})}{\partial \omega} = \sum_{k=1}^M V_k k t \cos(k\omega t + \varphi_k) \quad (9)$$

$$j_{2+k} = \frac{\partial h(\mathbf{x})}{\partial V_k} = \sin(k\omega t + \varphi_k) \quad (10)$$

$$j_{2+M+k} = \frac{\partial h(\mathbf{x})}{\partial \varphi_k} = V_k \cos(k\omega t + \varphi_k) \quad (11)$$

where  $k = 1, \dots, M$ .

The elements of the Jacobian are calculated from the estimates obtained in the step before, where the data belonging to the preceding data window were processed.

This approach requires the right choice of the sampling frequency, the length of the data window  $T_{\text{dw}}$ , and the initial guess for the vector of the unknown parameters  $\mathbf{x}_0$ . The initial vector  $\mathbf{x}_0$  can simply be calculated by using FFT. The number of iterations  $i$  from one data window can be reduced to one single iteration by setting  $i = 1$ . Through this, the estimate from the preceding iteration is used as input for the next iteration. This simplification significantly reduces the central processing unit requirements and at the same time does not influence the algorithm features. In [15], it is proven that the NTA algorithm has a second-order convergence. This feature allows us to set  $i = 1$ .

The presented NTA algorithm is adaptive in nature. That enables the provision of high measurement accuracy over a wide range of magnitude and frequency changes. With the initial guess  $\mathbf{x}_0$  correctly determined, the true estimates can be obtained in the frequency range from  $-f_s/2$  to  $+f_s/2$ . Given a step change of one (or all) model parameter(s), after a short convergence period  $t_{\text{cnv}}$ , the true estimates are obtained. The

convergence period is approximately equal to the size of the data window, i.e.,  $t_{\text{cnv}} \approx T_{\text{dw}}$ . Since the approach is based on the suitable linearization and on the ordinary Least Error Squares Estimation, it does not require *a priori* knowledge of the noise statistics as is required for optimal estimators [5], [6]. This is an important property, because it is often difficult to obtain reliable information about the noise statistics of the processed signal.

The described method requires relatively powerful micro-processors because the hardware organization is distributed over several processors. One processor is responsible for the online matrix inversion [see (6)], and the other processor can calculate the variables for the second algorithm stage. The accuracy of the method is of course restricted by the quality of A/D conversion.

### III. BASIC POWER COMPONENT DEFINITIONS AND TWO-STAGE NUMERICAL ALGORITHM DESCRIPTION

The power component definitions given in [11] are used in the algorithm.

For *single-phase systems*, the following representation can be used:

$$v = \sqrt{2}V_1 \sin(\omega t - \alpha_1) + \sqrt{2} \sum_{k \neq 1} V_k \sin(k\omega t - \alpha_k) \quad (12)$$

$$i = \sqrt{2}I_1 \sin(\omega t - \beta_1) + \sqrt{2} \sum_{k \neq 1} I_k \sin(k\omega t - \beta_k) \quad (13)$$

where  $k$  is the harmonics order. Through this, the rms values of voltages and currents are

$$V_{\text{RMS}} = \sqrt{V_1^2 + \sum_{k \neq 1} V_k^2} = \sqrt{V_1^2 + V_H^2} \quad (14)$$

$$I_{\text{RMS}} = \sqrt{I_1^2 + \sum_{k \neq 1} I_k^2} = \sqrt{I_1^2 + I_H^2}. \quad (15)$$

The active power is defined as

$$P = P_1 + P_H \quad (16)$$

where  $P_1$  is the fundamental (50 Hz or 60 Hz) active power

$$P_1 = V_1 I_1 \cos \theta_1 \quad (17)$$

and  $P_H$  is the harmonics active power

$$P_H = \sum_{k \neq 1} V_k I_k \cos \theta_k. \quad (18)$$

The fundamental reactive power is defined as

$$Q_1 = V_1 I_1 \sin \theta_1. \quad (19)$$

Budeanu's reactive power [16] is expressed as

$$Q_B = Q_1 + Q_H = Q_1 + \sum_{k \neq 1} V_k I_k \sin \theta_k \quad (20)$$

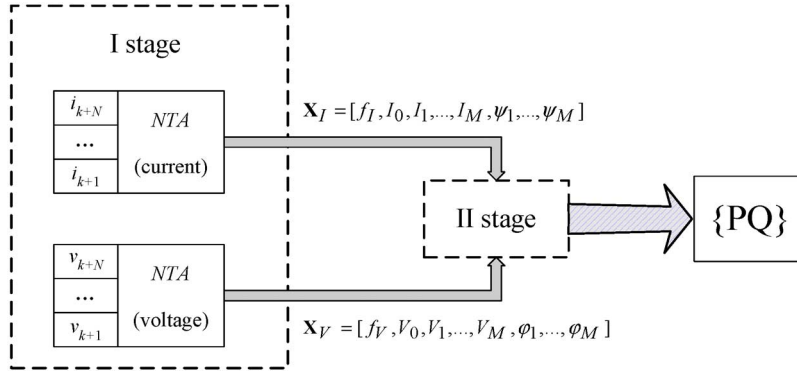


Fig. 1. Two-stage NTA algorithm for a single-phase system.

where  $\theta_k$  is the phase angle between  $V_k$  and  $I_k$ . Because of its inability to quantify the harmonic nonactive power flow [11], Budeanu's reactive power is not recommended to be used in engineering practice. The apparent power is defined as

$$S = V_{\text{RMS}} I_{\text{RMS}}. \quad (21)$$

The fundamental apparent power is defined as

$$S_1 = V_1 I_1. \quad (22)$$

From the energy flow point of view, the fundamental apparent, active, and reactive power components are of the highest interest. The nonfundamental power determined by the distortion of voltages and currents is defined as

$$S_N = \sqrt{S^2 - S_1^2}. \quad (23)$$

The nonactive power  $N$  can now be defined as

$$N = \sqrt{S^2 - P^2}. \quad (24)$$

In *three-phase systems*, in the general case (unbalanced and nonsinusoidal conditions), the voltages and currents in each phase ( $a, b, c$ ) could be represented by (12) and (13). By introducing the rms effective voltage and current in a three-wire system given as [11]

$$V_{e,\text{RMS}} = \frac{1}{3} \sqrt{V_{ab,\text{RMS}}^2 + V_{bc,\text{RMS}}^2 + V_{ca,\text{RMS}}^2} \quad (25)$$

$$I_{e,\text{RMS}} = \frac{1}{\sqrt{3}} \sqrt{I_{a,\text{RMS}}^2 + I_{b,\text{RMS}}^2 + I_{c,\text{RMS}}^2} \quad (26)$$

the effective three-phase apparent power is defined as

$$S_e = 3 \cdot V_{e,\text{RMS}} I_{e,\text{RMS}}. \quad (27)$$

The fundamental rms effective voltage and current are defined in a similar manner as

$$V_{e1,\text{RMS}} = \frac{1}{3} \sqrt{V_{ab1,\text{RMS}}^2 + V_{bc1,\text{RMS}}^2 + V_{ca1,\text{RMS}}^2} \quad (28)$$

$$I_{e1,\text{RMS}} = \frac{1}{\sqrt{3}} \sqrt{I_{a1,\text{RMS}}^2 + I_{b1,\text{RMS}}^2 + I_{c1,\text{RMS}}^2}. \quad (29)$$

The fundamental apparent power becomes

$$S_{e1} = 3 \cdot V_{e1,\text{RMS}} I_{e1,\text{RMS}}. \quad (30)$$

Having defined  $S_e$  and  $S_{e1}$ , the nonfundamental apparent power can be written as

$$S_{eN} = \sqrt{S_e^2 - S_{e1}^2}. \quad (31)$$

The total three-phase active power is the sum of the power per phase, i.e.,

$$P = P_a + P_b + P_c. \quad (32)$$

The power components given above are estimated by the two-stage NTA. In the first algorithm stage, the spectra and frequency of the processed voltages and currents are estimated, as described in the previous section. In Fig. 1, the voltage and current samples are labeled with  $v$  and  $i$ , respectively. It is assumed that data sampling is synchronized, and therefore, asynchronous A/D conversion has not been taken into account.

As output of the first algorithm stage, the voltage and current unknown parameter vectors, including frequency, harmonics magnitudes, and their phase angles, provide the input for the second algorithm stage. In Fig. 1, these vectors are denoted as  $\mathbf{x}_V$  and  $\mathbf{x}_I$ . Once the voltage and current parameters are known, it is relatively simple to calculate the power components in the second algorithm stage. In Fig. 1, the result of the second algorithm stage is denoted as  $\{PQ\}$ . In case of single-phase systems, the two-stage algorithm is shown in Fig. 1.

For three-phase systems, there are three blocks of the first algorithm stage, one for each phase.

#### IV. ALGORITHM TESTING

The two-stage NTA is tested with the help of computer-simulated tests (test signals with a known structure) and by using signals recorded under laboratory conditions. The computer-simulated tests are carried out for the sampling frequency  $f_s = 1600$  Hz and the data window size  $T_{\text{dw}} = 20$  ms.

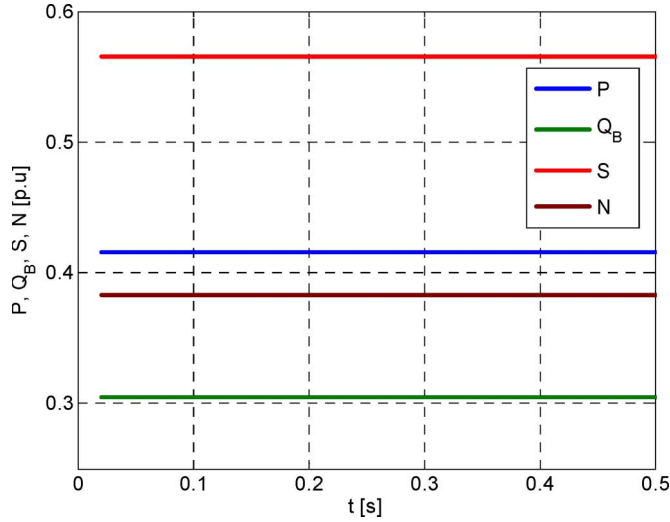


Fig. 2. Estimated power components (static test).

### A. Static Tests

The following input signals are processed:

$$v(t) = \cos(\omega t + 30^\circ) + 0.3 \cos(3\omega t + 90^\circ) + 0.2 \cos(5\omega t + 150^\circ) \quad (33)$$

$$i(t) = \cos(\omega t) + 0.3 \cos(3\omega t) + 0.2 \cos(5\omega t). \quad (34)$$

In Fig. 2, the estimated power components are shown. The following accurate results are obtained:  $P = 0.41569$  p.u.,  $Q_B = 0.305$  p.u.,  $S = 0.565$  p.u., and  $N = 0.38266$  p.u.. The highest relative error for static testing was smaller than  $10^{-5}\%$ , and this was because of the finite precision of the computer number representation.

Using the same input signals [(33) and (34)], but distorted with an additive zero-mean Gaussian random noise with SNR = 70 dB, the unknown power components are estimated and shown in Fig. 3. (The SNR is defined as

$$\text{SNR} = 20 \log \frac{S}{\sqrt{2}\sigma} \quad (35)$$

where  $S/\sqrt{2} = S_{\text{RMS}}$  is the root mean square value of the processed signal, and  $\sigma$  is the standard deviation of the noise.) In this test, the estimated values slightly differ from the exact values presented in Fig. 2.

The algorithm sensitivity to random noise is determined by the selection of the data window size ( $T_{\text{dw}}$ ). For an increased data window size, the sensitivity to noise decreases and vice versa. On the other hand, by increasing the data window size, the algorithm convergence is prolonged so a compromise in data window size must be found. The constraints are the quality of the processed signals and the dynamic properties of the monitored process. In Fig. 4, the maximal active power relative errors versus the SNR are depicted. It is obvious that the wider is the data window, the lower is the maximal error.

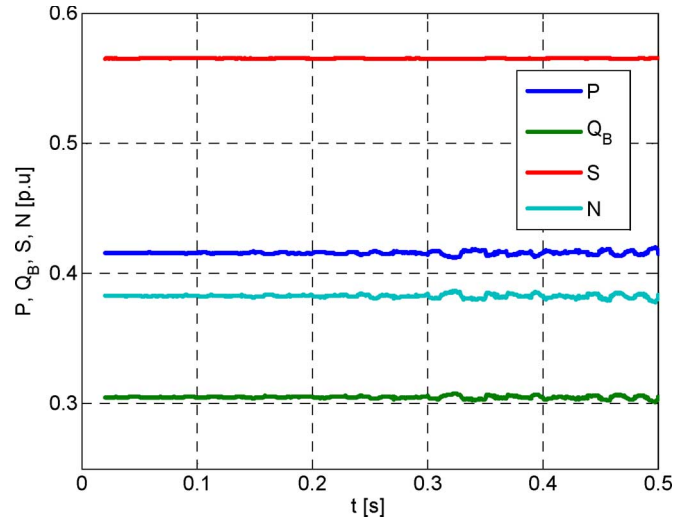


Fig. 3. Estimated power components in the presence of random noise.

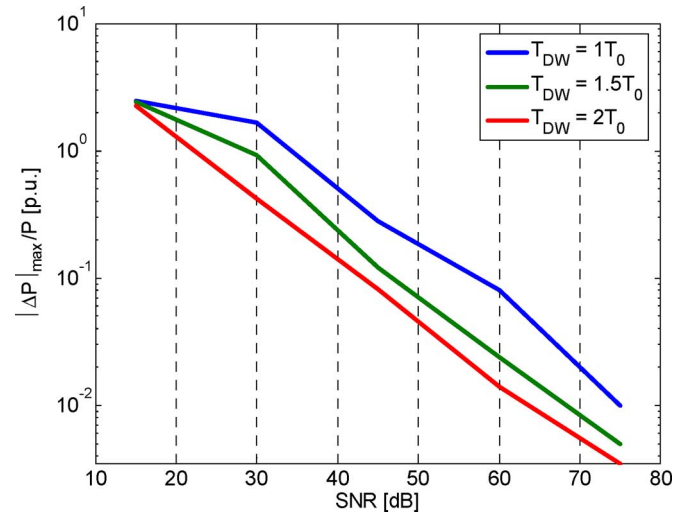


Fig. 4. Maximal error versus SNR and data window width.

### B. Dynamic Tests

The dynamic properties and the sensitivity to frequency deviations are verified by processing the following distorted voltage and current signals:

$$v(t) = \cos(\omega t + 45^\circ) + 0.5 \cos(3\omega t + 120^\circ) + 0.3 \cos(5\omega t + 150^\circ) + 0.2 \cos(7\omega t + 280^\circ) \quad (36)$$

$$i(t) = \cos(\omega t) + 0.4 \cos(3\omega t + 60^\circ) + 0.2 \cos(5\omega t + 30^\circ) + 0.1 \cos(7\omega t + 130^\circ). \quad (37)$$

To verify the dynamic properties of the proposed algorithm, in the period from  $t = 0$  to 0.158 s, both test signals were pure cosine signals and consisted of the first terms from (36) and (37). At  $t = 0.158$  s, both input signals are distorted with higher harmonics as given by (36) and (37). Simultaneously, the frequency of the fundamental harmonic is instantaneously changed from 50 to 45 Hz. In Figs. 5 and 6, the estimated power components and frequency are respectively depicted. In the period before the distortion is applied,  $S = 0.5$  p.u., and  $P = Q = N = 0.5/\sqrt{2} = 0.35355$  p.u. (see Fig. 5).

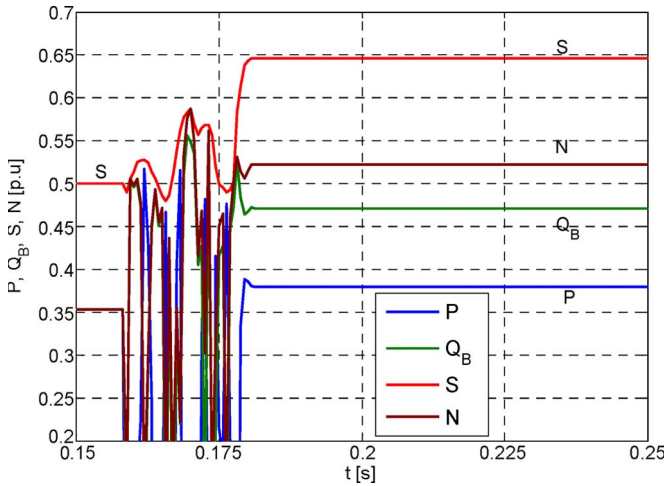


Fig. 5. Estimated power components (dynamic test) by the NTA algorithm.

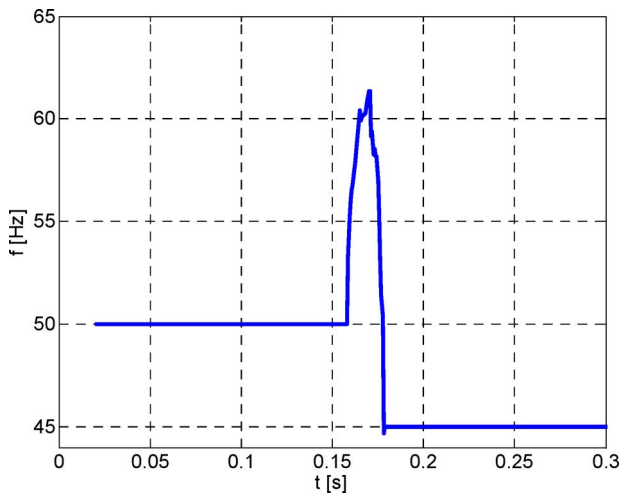


Fig. 6. Frequency estimates (dynamic test).

After a convergence period of  $t_{cnv} = 0.02$  s, true estimates of the new power components are obtained ( $P = 0.3799$  p.u.,  $Q_B = 0.4711$  p.u.,  $S = 0.6461$  p.u., and  $N = 0.5226$  p.u.). The same is valid for the estimated frequency (see Fig. 6). The length of the data window determines the algorithm convergence properties. For the shorter data window sizes, one obtains the faster convergence and vice versa. The highest relative error obtained in power component measurement during dynamic testing was less than  $10^{-5}\%$  (not including the convergence period).

In Fig. 7, the results of processing the dynamic signals obtained by using the FFT algorithm are presented. Before the distortion of the input signals, both algorithms give identical results. However, for  $t > 0.158$  s, as a consequence of the frequency changes, the FFT algorithm gives erroneous results.

C. Laboratory Testing

In the next example, the signals recorded under laboratory conditions are used for the evaluation of the NTA algorithm.

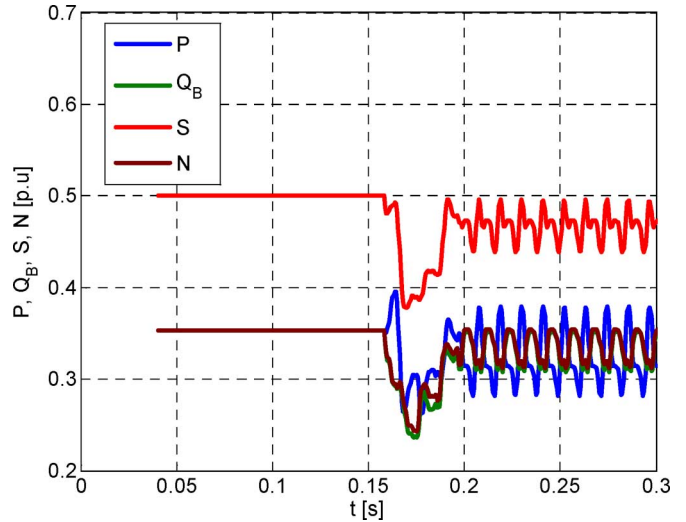


Fig. 7. Estimated power components obtained by the FFT algorithm.

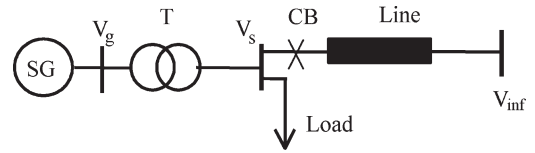


Fig. 8. Laboratory setup (synchronization of two networks).

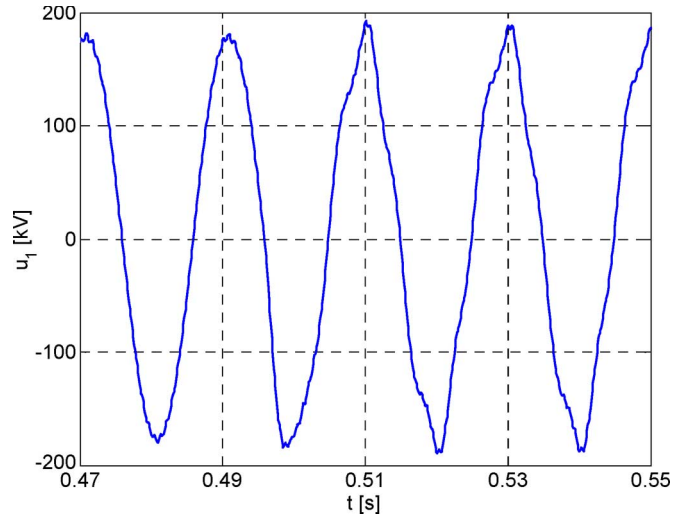


Fig. 9. Phase a voltage before and after synchronization.

For this case, the synchronization of two networks is used as an attractive example.

The synchronization of two networks is a normal and standard procedure for system operators in a multimachine power system. Often, a single generator unit is synchronized to the rest of the system. To avoid overcurrents, tripping of protective devices, instability, or any other damage, the synchronization has to be carefully done. For a successful synchronization, the corresponding phasors of the two systems are approximately the same (equal amplitudes, phase angles, and frequencies). Nowadays, synchronization is automatically done by digital devices. For the next test, a successful synchronization is taken in the laboratory at Saarland University (Germany). For this, a modern data acquisition digital system [17] was used.

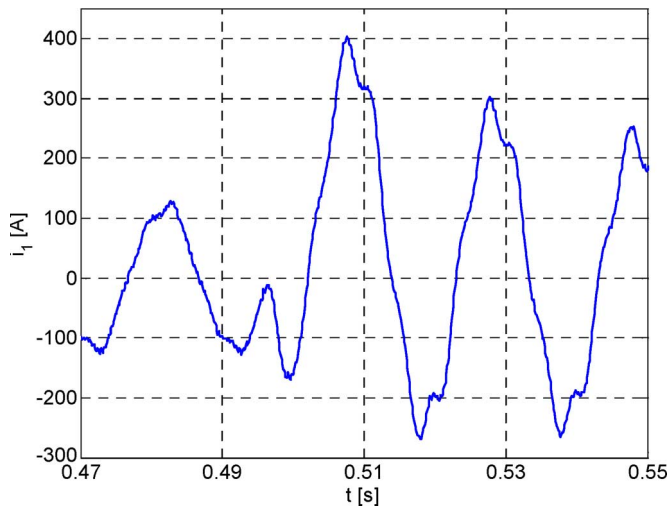


Fig. 10. Phase a current before and after synchronization.

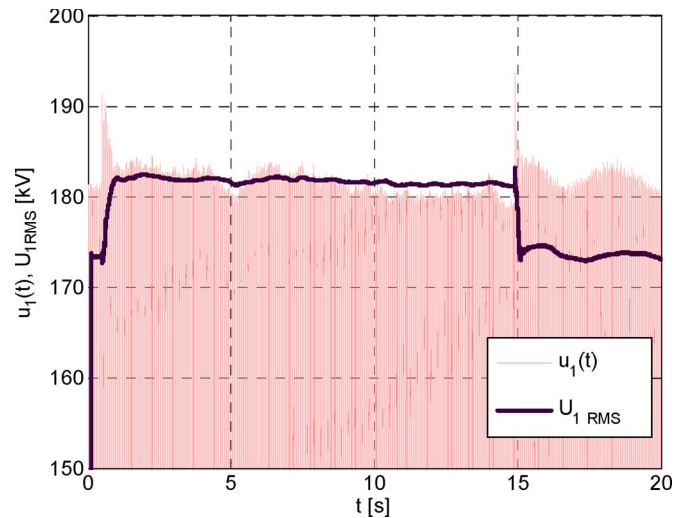


Fig. 12. Voltage and its estimated amplitude.

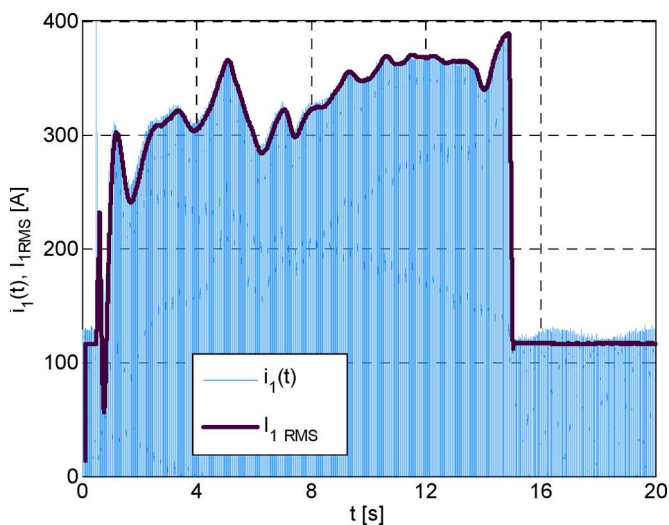


Fig. 11. Current and its estimated amplitude.

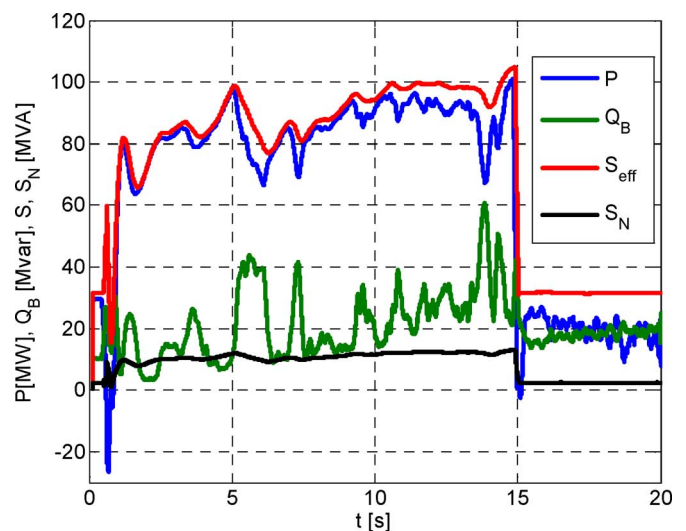


Fig. 13. Estimated generator power components.

In Fig. 8, a single-line diagram of a synchronous generator (SG) connected over a block transformer (T) to the load is shown. By closing the circuit breaker (CB) at  $t = 0.495$  s, the single generator system is synchronized with the infinite bus  $V_{inf}$ . At  $t = 15$  s, the two networks are separated. In the test example, the generator voltages and currents were sampled with 5 kHz in a data window of 120 ms.

In Figs. 9 and 10, the voltage and current signals just before and after the synchronization are shown, and both signals are distorted. The total harmonic distortion of the current signals is about 8%. The harmonic distortion for the voltage was 1%–2% before synchronization, 8%–10% in the period of synchronized operation of the two systems, and 1%–2% after the disconnection from the infinite bus.

However, the synchronization was successful, but the context was far from ideal. The corresponding phasors and the frequencies of the two subsystems were not the same at the time of synchronization. As a consequence, a transient process takes place. During this transient phase, the currents are dramatically increased, the voltages are distorted, and the frequency oscil-

lates. In this period of time, generator torsion oscillations occur because of the fact that the synchronization was not ideal.

In Figs. 11 and 12, the estimated amplitudes of the voltage and current signals as well as those instantaneous values are shown.

Based on the parameters estimated in the first algorithm stage, the unknown power components (active ( $P$ ), Budeanu’s reactive ( $Q_B$ ), effective apparent ( $S_{eff}$ ), and nonfundamental apparent ( $S_N$ ) power) and the frequency are estimated in the second algorithm stage (see Figs. 13 and 14).

## V. CONCLUSION

In this paper, a new two-stage NTA algorithm for the digital metering of power components according to IEEE Standard 1459-2000 is presented and tested in detail. It is based on the application of the NTA, which is a nonlinear nonrecursive estimator suitable for the estimation of the power spectrum. It has been shown that the algorithm is not sensitive to frequency changes of the distorted input signal. The algorithm has been tested using static and dynamic computer-simulated tests, as well as under laboratory conditions (synchronization

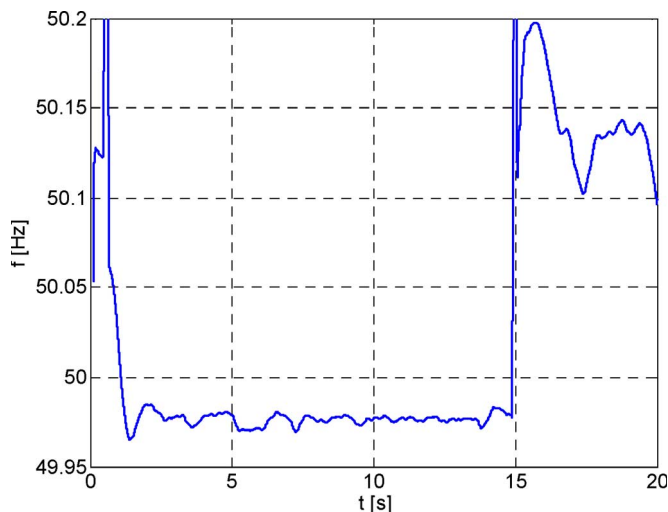


Fig. 14. Estimated generator frequency.

of two active networks). The obtained results confirm the high accuracy of the algorithm. Through the comparison with the FFT algorithm, it has been proved that it is superior during off-nominal frequency conditions. The fast algorithm convergence offers the opportunity to apply the algorithm in processes where fast and very fast transients can occur. The technique is not limited to measurement applications in power systems only. It might also be applied in designing algorithms for other applications.

#### REFERENCES

- [1] A. Girgis *et al.*, "Measurement and characterization of harmonics and high frequency distortion for a large industrial load," *IEEE Trans. Power Del.*, vol. 5, no. 1, pp. 427–434, Jan. 1990.
- [2] R. Arseneau *et al.*, "A survey of north American electric utility concerns regarding nonsinusoidal waveforms," *IEEE Trans. Power Del.*, vol. 11, no. 1, pp. 73–78, Jan. 1996.
- [3] A. V. Oppenheim and R. Schaffer, *Digital Signal Processing*. Englewood Cliffs, NJ: Prentice-Hall, Jan. 1975.
- [4] C. Gherasim *et al.*, "DSP implementation of power measurements according to the IEEE trial-use Standard 1459," *IEEE Trans. Instrum. Meas.*, vol. 53, no. 4, pp. 1086–1092, Aug. 2004.
- [5] A. Girgis and J. Qui, "Measurement of the parameters of slowly time varying high frequency transients," *IEEE Trans. Instrum. Meas.*, vol. 38, no. 6, pp. 1057–1063, Dec. 1989.
- [6] P. K. Dash *et al.*, "An extended complex Kalman filter for frequency measurement of distorted signals," *IEEE Trans. Instrum. Meas.*, vol. 49, no. 4, pp. 746–753, Aug. 2000.
- [7] S. Fryze, "Wirk-, Blind- und Scheinleistung in elektrischen Stromkreisen mit nichtsinusförmigem Verlauf von Strom und Spannung," *Elektrotech. Z.*, vol. 25, pp. 569–599, Jun. 1932.
- [8] L. S. Czarnecki, "Energy flow and power phenomena in electrical circuits: Illusions and reality," *Elect. Eng.*, vol. 82, no. 4, pp. 119–126, 2000.
- [9] A. E. Emanuel, "On the definition of power factor and apparent power in unbalanced polyphase circuits with sinusoidal voltage and currents," *IEEE Trans. Power Del.*, vol. 8, no. 3, pp. 841–852, Jul. 1993.
- [10] P. S. Filipinski, "Apparent power—A misleading quantity in the nonsinusoidal power theory: Are all nonsinusoidal power theories doomed to fail?" *Eur. Trans. Elect. Power (ETEP)*, vol. 3, pp. 21–26, 1993.
- [11] *Definitions for the Measurement of Electric Quantities Under Sinusoidal, Nonsinusoidal, Balanced, or Unbalanced Conditions*, IEEE Std. 1459-2000, Jan. 2000.
- [12] J. L. Willems, J. A. Ghijsels, and A. E. Emanuel, "The apparent power concept and the IEEE Standard 1459-2000," *IEEE Trans. Power Del.*, vol. 11, no. 1, pp. 73–78, Jan. 1996.
- [13] A. E. Emanuel, "Summary of IEEE Standard 1459: Definitions for the measurement of electric power quantities under sinusoidal, nonsinusoidal, balanced, or unbalanced conditions," *IEEE Trans. Ind. Appl.*, vol. 40, no. 3, pp. 869–876, May/Jun. 2004.
- [14] V. Terzija, M. Djuric, and B. Kovacevic, "Voltage phasor and local system frequency estimation using Newton type algorithm," *IEEE Trans. Power Del.*, vol. 9, no. 3, pp. 1368–1374, Jul. 1994.
- [15] V. Terzija and M. Djuric, "Direct estimation of voltage phasor, frequency and its rate of change using Newton's iterative method," *J. Elect. Power Energy Syst.*, vol. 16, no. 6, pp. 423–428, 1994.
- [16] C. I. Budeanu, *Puissance Reactives at Fictives*. Bucharest, Romania: Institut Romain de l'Energie, 1927. Publ. 2.
- [17] *IMC-μ-Musyscs*. [Online]. Available: [www.imc-berlin.de/messtechnik](http://www.imc-berlin.de/messtechnik)



**Vladimir V. Terzija** (M'95–SM'00) received the Dipl.-Ing., M.Sc., and Ph.D. degrees from the University of Belgrade, Belgrade, Serbia.

From 1997 to 1999, he was an Assistant Professor with the University of Belgrade. He was a Humboldt Research Fellow with Saarland University, Saarland, Germany, in 1999. From 2000 to 2006, he was with ABB AG, Mannheim, Germany, as an expert for switchgears and distribution automation. Since 2006, he has been the Engineering and Physical Sciences Research Council (EPSRC) Chair Professor in power system engineering with the School of Electrical and Electronic Engineering, University of Manchester, Manchester, U.K. His main research interests are applications of intelligent methods to power system monitoring, control, and protection, as well as switchgears and DSP applications in power systems.



**Vladimir Stanojević** received the Dipl.-Ing. and M.S. degrees from the University of Belgrade, Belgrade, Serbia.

From 1998 to 2005, he was a Power System Operation Engineer with the Electric Power Industry of Serbia. In 2001, he was an Associated Research Fellow with the Korea Electrotechnology Research Institute, Changwon, Korea. From 2005 to 2006, he was a Remote Data Acquisition Engineer with the Department of Measuring and Accounting of Data, Serbian TSO. Since 2006, he has been a Research Assistant with the Imperial College London, London, U.K. His fields of interest are power quality, electromechanical transient processes, and DSP applications in power systems.



**Marjan Popov** (M'95–SM'03) received the Dipl.-Ing. and M.S. degrees in electrical engineering from St. Cyril and Methodius University, Skopje, Macedonia, in 1993 and 1998, respectively, and the Ph.D. degree from Delft University of Technology (TU Delft), Delft, The Netherlands, in 2002.

From 1993 to 1998, he was a Teaching and Research Assistant with the Faculty of Electrical Engineering, University of Skopje. In 1997, he was an academic visitor with the University of Liverpool, Liverpool, U.K. He is currently with the Power System Laboratory, TU Delft, where he is an Assistant Professor with the group of electrical power systems. His major fields of interest are arc modeling, transients in power systems, parameter estimation, and relay protection.



**Lou van der Sluis** (M'81–SM'86) was born in Geervliet, The Netherlands, on July 10, 1950. He received the M.Sc. degree in electrical engineering from Delft University of Technology, Delft, The Netherlands, in 1974.

In 1977, he was a Test Engineer with the High Power Laboratory, KEMA, Arnhem, The Netherlands, and was involved in the development of a data acquisition system, computer calculations of test circuits, and the analysis of test data by digital computer. He was a part-time Professor in 1990 and has been a full-time Professor since 1992 with the Power Systems Department, Delft University of Technology. He was the Chairman of CC-03 of Cigre and Cired to study the transient recovery voltages in medium- and high-voltage networks. He is currently a member of Cigre WG A3-20 for modeling power system components.